Available online at www.sciencedirect.com
SCIENCE DIRECT®
International Journal of Mass Spectrometry 244 (2005) 84–90
International Journal of Mass Spectrometry
www.elsevier.com/locate/ijms

Rate estimates for collisions of ionic clusters with neutral reactant molecules

Grit Kummerlöwe, Martin K. Beyer *

Department Chemie, Physikalische Chemie 2, Technische Universität München, Lichtenbergstraße 4, 85747 Garching, Germany

Received 10 March 2005; received in revised form 14 March 2005; accepted 14 March 2005

Abstract

Measured reaction rate constants of ionic clusters often exceed the collision rate calculated with the widely used Average Dipole Orientation (ADO) theory. Accurate trajectory calculations, however, are in most cases not possible since detailed information on the cluster geometry and the interaction potential with the neutral is not readily available. Two simple and universally applicable models to estimate these collision rates are presented here. In both models, the cluster and the neutral reaction partner are treated as hard spheres, and the charge is treated as a point charge. The attraction between the point charge and the neutral molecule is described with the interaction potential from ADO theory. For the Hard Sphere Average dipole orientation (HSA) collision rate, the charge is located in the center of the cluster, while in the Surface Charge Capture (SCC) model, the charge is drawn to the cluster surface by the attractive interaction with the neutral collision partner. Both models lead to significantly increased collision rate constants, in comparison with Langevin or ADO capture rates and purely geometric hard-sphere collisions. For weakly polarizable clusters like $(H_2O)_n^-$, the newly derived HSA rate constants lie close to experimentally measured rate constants. For the reactions of metal clusters with CO, the SCC model is in surprisingly good agreement with experiment. Although both models are far from being exact theories, they seem valuable for the interpretation of gas phase reactivity experiments of ionic clusters.

Keywords: Capture theory; Cluster; Collision rate; Gas phase reaction

1. Introduction

In gas phase ion chemistry, the collision rate between the ion and a neutral reactant forms the upper theoretical limit for the reaction rate constant. This rate is frequently calculated with the help of average dipole orientation (ADO) theory as developed by Su and Bowers [1,2], which includes the Langevin rates for the capture of a non-polar neutral molecule by an ion [3]. ADO theory is based on the classical trajectory of a linear dipole in the field of a point charge, which is the standard approach for the theoretical investigation of capture processes [4–7]. The effect of the ion size on the rate constant was considered for protonated alkanes up to $C_4H_9^+$, and found to be insignificant [8].

In ion mobility experiments, on the other hand, a hard-sphere collision model is commonly employed [9–12]. The effect of the long-range potential has been considered in some cases [13,14], and it was concluded for fullerenes with 20–60 carbon atoms that the effect on the calculated mobility was smaller than 10% at room temperature [13]. Recent work on the mobility of mixed $Ag_mAu_n^+$ clusters by Kappes and co-workers [15] showed that perfect agreement between experimental and theoretical cross sections can be reached if the charge-induced dipole interaction between the cluster and the buffer gas atom is modelled with an accurate charge distribution in a classical trajectory model.

The shortcomings of ADO theory have been overcome by a number of theoretically rigorous approaches like classical trajectory calculations and adiabatic channel capture models [16–23]. The current work goes into a different direction, seeking a generally applicable way of estimating collision rates in ion–molecule reactions of ionic clusters. It was

* Corresponding author. Tel.: +49 89 289 13417; fax: +49 89 289 13416.
E-mail address: beyer@ch.tum.de (M.K. Beyer).

1387-3806/$ – see front matter © 2005 Elsevier B.V. All rights reserved.
doi:10.1016/j.ijms.2005.03.012

motivated by the measurement of rate constants, which exceeded the theoretical ADO rate by up to a factor of four [24,25]. An error of 25% is in general accepted for the absolute measured rate constant in ICR experiments, which is almost entirely due to the uncertainty of the pressure measurement inside the ICR cell [26,27]. The large deviation in the cluster studies indicates that the application of ADO theory is no longer justified for larger clusters, but clearly for other reasons than the ones treated and overcome in the refined theories mentioned above. A detailed trajectory calculation, however, as employed in the refined ion mobility measurements [13–15], is in general not possible in the reactivity studies. The cluster geometries and exact charge distribution are in most cases unknown, and the interaction of the cluster ion with the reaction gas is much more complicated than with the helium buffer gas in ion mobility studies.

Here, we present two modified versions of classical capture theory, which account for the finite size of the cluster. In both approaches, the cluster and the neutral reaction partner are treated as hard spheres, and the charge is treated as a point charge. The attraction between the point charge and the neutral molecule is described with the interaction potential from ADO theory. Although ADO theory has been shown to have some shortcomings, as outlined above, the assumptions which have to be made for the geometry and charge distribution of the cluster introduce an error into the calculations which is much larger than the one introduced by using ADO theory.

The two models differ in the location of the charge. In the Hard Sphere Average dipole orientation (HSA) model, the charge is fixed in the center of the spherical cluster. In the Surface Charge Capture (SCC) model, the charge is drawn to the cluster surface by the attractive interaction with the neutral collision partner. At the point of closest approach, the charge is in closest possible proximity to the neutral collision partner. Both models are compared with previously published experimental results on metal cluster and water cluster reaction rate constants.

2. Theoretical models

2.1. Hard Sphere Average dipole orientation (HSA) theory

Fig. 1 illustrates three different types of collisions between a neutral molecule and an idealized spherical cluster. If the cluster is neutral, Fig. 1a, the molecule collides if the impact parameter is smaller than b_g, which defines the hard-sphere cross section $\sigma_g = \pi b_g^2$.

If the radius of a charged cluster is smaller than the ADO capture radius, Fig. 1b, the collision cross section can be described by ADO theory. If the radius of a charged cluster, however, is larger than the ADO capture radius, Fig. 1c, a neutral molecule may be deflected sufficiently to collide with

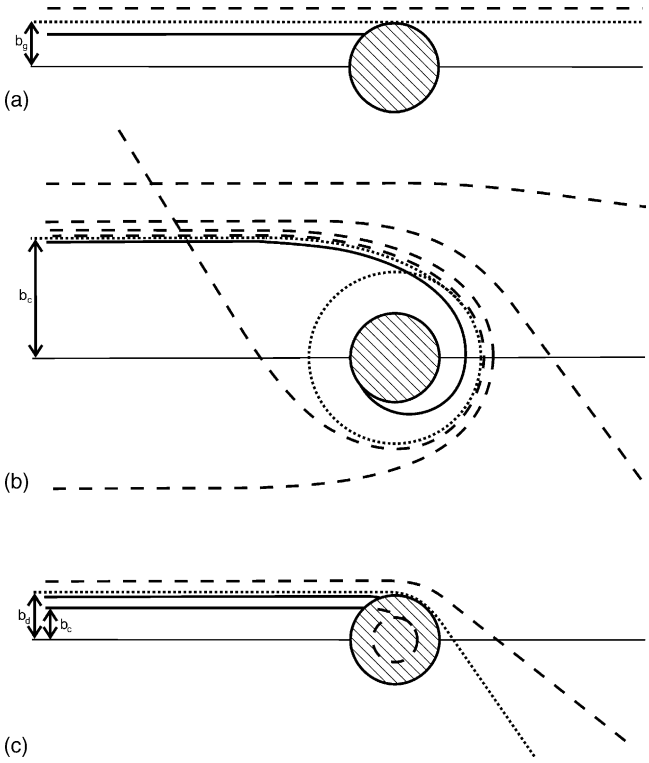

Fig. 1. Three types of collisions of a neutral molecule with a spherical cluster. (a) The cluster is also neutral. The trajectory of the molecule is linear, a collision occurs if the impact parameter b is smaller than b_g. (b) The cluster is charged and smaller than the sphere defined by the classical capture radius from ADO theory. b_c is the maximum impact parameter for which the molecule is captured. A collision occurs if $b \leq b_c$. (c) The cluster is charged and larger than the sphere described by the capture radius. If $b > b_c$, the molecule is not captured, but still deflected by the attractive interaction. A collision occurs if the closest approach occurs at a distance smaller than b_g. The maximum impact parameter b_d corresponds to the trajectory where the closest approach equals b_g.

the cluster, without being captured. We call this a hard-sphere deflection (HSD) collision. In this case, the maximum impact parameter is larger than the geometric impact parameter from Fig. 1a, $b_d > b_g$.

The capture radius is velocity dependent, therefore there is a contribution of ADO capture and HSD collisions for any cluster of finite size. The contribution of ADO capture, however, will be larger for lower temperatures and smaller clusters. In order to calculate the total collision rate, we have to calculate the impact parameter $b_d(v)$ and the critical velocity v_c at which the cross section calculation changes from ADO theory to the HSD cross section $\sigma_{HSD} = \pi b_d^2$.

As outlined in detail before by Su and Bowers [1], the interaction of the neutral molecule and the charged cluster is described with an effective potential $V_{eff}(r)$, which accounts for the conservation of angular momentum in the system:

$$V_{eff}(r) = \frac{\mu v^2 b^2}{2r^2} - \frac{\alpha q^2}{32\pi^2 \varepsilon_0^2 r^4} - \frac{c\mu_D q}{4\pi\varepsilon_0 r^2} \quad (1)$$

Here, μ is the reduced mass of the molecule and the cluster, v their relative velocity, b the impact parameter, r the distance between the center of the cluster and the center of the molecule, q the cluster charge, and ε_0 the vacuum permittivity. The neutral molecule is described by its polarizability α, its dipole moment μ_D and the dipole locking constant c introduced by Su and Bowers [8].

According to Langevin [3], the capture radius r_c is given by the two conditions $\partial V_{eff}/\partial r = 0$ and $E_r = V_{eff}$, with the total kinetic energy E_r in the system:

$$E_r = \frac{1}{2}\mu v^2 \tag{2}$$

$$\frac{\partial V_{eff}(r)}{\partial r} = 0 = -\frac{\mu v^2 b_c^2}{r_c^3} + \frac{\alpha q^2}{8\pi^2\varepsilon_0^2 r_c^5} + \frac{c\mu_D q}{2\pi\varepsilon_0 r_c^3} \tag{3}$$

$$V_{eff}(r_c) = E_r = \frac{\mu v^2 b_c^2}{2r_c^2} - \frac{\alpha q^2}{32\pi^2\varepsilon_0^2 r_c^4} - \frac{c\mu_D q}{4\pi\varepsilon_0 r_c^2} = \frac{1}{2}\mu v^2 \tag{4}$$

Equations (3) and (4) yield the capture radius r_c:

$$r_c = \sqrt[4]{\frac{\alpha q^2}{16\pi^2\varepsilon_0^2\mu v_c^2}} \tag{5}$$

The critical velocity v_c for the transition from the ADO to the HSD collision regime is reached if $r_c = b_g$:

$$v_c = \sqrt{\frac{\alpha q^2}{16\pi^2\varepsilon_0^2\mu b_g^4}} \tag{6}$$

For $v \le v_c$, the collision rate is calculated with ADO theory [1,8]:

$$k_{ADO}(v) = \frac{q}{2\varepsilon_0\sqrt{\mu}}\left(\sqrt{\alpha} + \frac{c\mu_D}{\sqrt{\mu}v}\right) \tag{7}$$

In the HSD collision regime, $v > v_c$, we have to calculate b_d for which the minimum distance between the molecule and the cluster on the trajectory amounts to b_g, which allows a hard-sphere collision. In an attractive potential, the relation between b_d and b_g is given as [28]:

$$1 - \frac{b_d^2}{b_g^2} = \frac{V(b_g)}{E_r} \tag{8}$$

We use again $V(r)$ as derived in ADO theory [1,8] to calculate b_d as a function of v and b_g from (2), (8) and (9):

$$V(r) = -\frac{\alpha q^2}{32\pi^2\varepsilon_0^2 r^4} - \frac{c\mu_D q}{4\pi\varepsilon_0 r^2} \tag{9}$$

$$b_d(v) = \sqrt{b_g^2 + \frac{\alpha q^2}{16\pi^2\varepsilon_0^2\mu v^2 b_g^2} + \frac{c\mu_D q}{2\pi\varepsilon_0\mu v^2}} \tag{10}$$

This translates into the hard-sphere deflection cross section $\sigma_{HSD}(v)$ and rate constant $k_{HSD}(v)$:

$$\sigma_{HSD}(v) = \pi b_d^2 = \pi b_g^2 + \frac{\alpha q^2}{16\pi\varepsilon_0^2\mu v^2 b_g^2} + \frac{c\mu_D q}{2\varepsilon_0\mu v^2} \tag{11}$$

$$k_{HSD}(v) = \sigma_{HSD}(v)v = \pi v b_g^2 + \frac{\alpha q^2}{16\pi\varepsilon_0^2\mu v b_g^2} + \frac{c\mu_D q}{2\varepsilon_0\mu v} \tag{12}$$

Equation (11) shows that the geometric cross section πb_g^2 is enlarged by the deflection of the particle towards the charged cluster. The total collision rate k_{HSA} is obtained by convoluting the ADO and HSD rate constants with the Maxwell distribution $f(v)$:

$$k_{HSA} = \int_0^{v_c} k_{ADO} f(v)\,dv + \int_{v_c}^{\infty} k_{HSD} f(v)\,dv \tag{13}$$

$$f(v) = 4\pi v^2\left(\frac{\mu}{2\pi k_B T}\right)^{3/2} \exp\left(-\frac{\mu v^2}{2k_B T}\right) \tag{14}$$

Equation (13) has to be integrated numerically.

2.2. Surface Charge Capture (SCC) theory

In an ideally conducting cluster, the point charge may move freely within the geometric boundaries of the cluster. In this case, the approaching neutral molecule will draw the charge to the cluster surface. The collision rate is in this case estimated as illustrated in Fig. 2. The charge is fixed to the point on the surface where the neutral molecule has its closest approach to the cluster. If the neutral molecule is captured by the charge, it will inevitably collide with the cluster surface. The impact parameter b_{SCC} then amounts to:

$$b_{SCC}(v) = r_{cluster} + b_c(v) \tag{15}$$

with

$$b_c(v) = \frac{\sqrt{k_{ADO}(v)}}{\pi v} \tag{16}$$

Numeric convolution of the cross section with the Maxwell distribution again yields the SCC collision rate k_{SCC}:

$$k_{SCC} = \int_0^{\infty} \pi b_{SCC}^2(v) v f(v)\,dv \tag{17}$$

Obviously, this treatment is not exact, since deflections similar to the HSA case which do not result in capture may still lead to a collision, and the charge is not localized in the center of mass of the cluster. Another simplification is that the charge moves across the cluster surface during the approach of the neutral collision partner, and thus the interaction is slightly underestimated. Both effects, if treated correctly, would lead to some increase of the calculated collision rate. However, given the overall crudeness of the approach, the SCC rate is meant to allow a semiquantitative interpretation of the measured reaction rates.

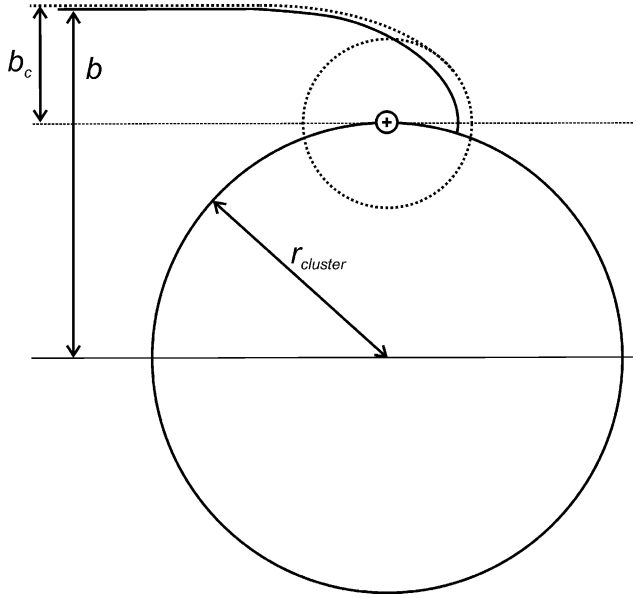

Fig. 2. Derivation of the Surface Charge Capture (SCC) rate. The interaction with the approaching neutral molecule shifts the charge to the surface of the cluster. For the calculation it is assumed that the charge is fixed in the position indicated in the figure. If the neutral collision partner is captured by the surface charge, it will collide with the cluster. The maximum collision impact parameter is given as the sum of the cluster radius $r_{cluster}$ and the capture impact parameter b_c.

3. Examples

The principal difficulty in the application of these models is a reasonable estimate for b_g, i.e., the size of the cluster and the neutral collision partner. Ideally, this estimate is generally applicable. We assume that the spherical cluster of composition $X_n^{\pm}$ has the same density ρ as the bulk material. The radius of the cluster $r_{cluster}$ can then be calculated from its mass nm_X, where m_X denotes the mass of the monomer:

$$r_{cluster} = \sqrt[3]{\frac{3nm_X}{4\pi\rho}} \tag{18}$$

The radius of the neutral molecule $r_{molecule}$ can be derived from the viscosity η of the gas [28]:

$$r_{molecule} = \frac{1}{8}\sqrt[4]{\frac{25m_{molecule}k_BT}{\pi\eta^2}} \tag{19}$$

This yields the desired value b_g:

$$b_g = r_{cluster} + r_{molecule} \tag{20}$$

The geometric cross section $\sigma_g = \pi b_g^2$ can also be used to calculate the rate constant k_g of a purely geometric collision as displayed in Fig. 1a:

$$k_g = \int_0^\infty \sigma_g v f(v)\,dv = \pi b_g^2 \int_0^\infty v f(v)\,dv = \pi b_g^2 \sqrt{\frac{8k_BT}{\pi\mu}} \tag{21}$$

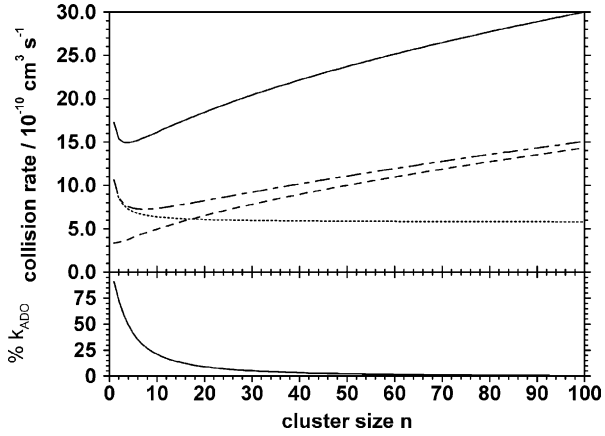

Fig. 3. Collision $(H_2O)_n^- + CO_2$. *Upper panel*: Hard sphere ADO rate k_{HSA} (dot-dashed line), Surface Charge Capture rate k_{SCC} (solid line), classical ADO collision rate k_{ADO} (dotted line), and geometric collision rate k_g (dashed line). Starting around $n = 5$, k_{HSA} deviates significantly from k_{ADO}, and from $n = 10$ runs almost parallel to k_g. With increasing size, k_{HSA} converges slowly against k_g. At $n = 100$, k_{HSA} is still 5% larger than k_g. k_{SCC} is consistently about twice as high as k_{HSA}. *Lower panel*: Fraction of molecules with $v \le v_c$, whose collision rate is calculated with classical ADO capture theory. Even at a cluster sizes of $n = 30$, 5% of the molecules are so slow that their capture radius is larger than the cluster.

This approach was used to calculate the HSA collision rates k_{HSA} and SCC collision rates k_{SCC} for singly charged water clusters with CO_2, as well as for singly charged platinum clusters with CO and He, in the cluster size region $n = 1$–100 at room temperature. The results are displayed in Figs. 3–5, with the ADO rate k_{ADO} and the purely geometric collision rate k_g shown for comparison (Source code and

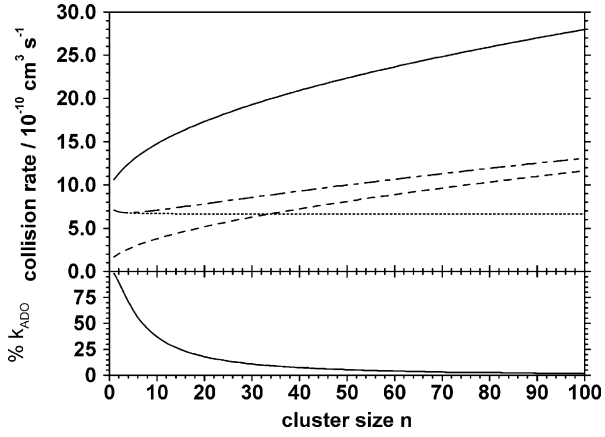

Fig. 4. Collision $Pt_n^{\pm} + CO$. *Upper panel*: Hard sphere ADO rate k_{HSA} (dot-dashed line), Surface Charge Capture rate k_{SCC} (solid line), classical ADO collision rate k_{ADO} (dotted line), and geometric collision rate k_g (dashed line). Starting around $n = 5$, k_{HSA} deviates significantly from k_{ADO}, and almost immediately runs parallel to k_g. With increasing size, k_{HSA} converges very slowly against k_g. At $n = 100$, k_{HSA} is still 12.5% larger than k_g. k_{SCC} is consistently about twice as high as k_{HSA}. *Lower panel*: Fraction of molecules with $v \le v_c$, whose collision rate is calculated with classical ADO capture theory. Only above a cluster sizes of $n = 50$, fewer than 5% of the molecules are slow enough that their capture radius is larger than the cluster. This reflects the strong interaction of the polar CO molecule with the charged cluster.

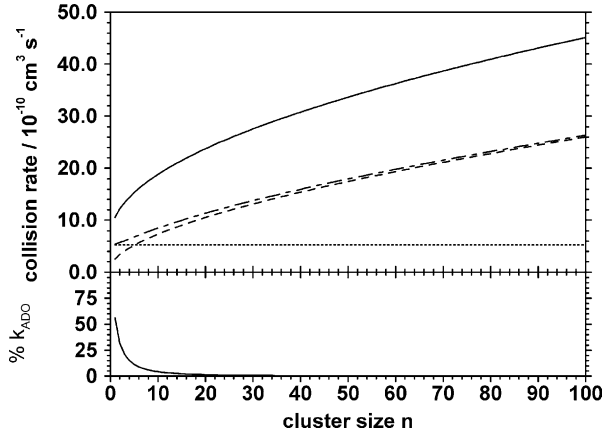

Fig. 5. Collision $Pt_n^{\pm}$ + He. *Upper panel*: Hard sphere ADO rate k_{HSA} (dot-dashed line), Surface Charge Capture rate k_{SCC} (solid line), classical ADO collision rate k_{ADO} (dotted line), and geometric collision rate k_g (dashed line). Already for $n = 2$, k_{HSA} deviates significantly from k_{ADO}, and almost immediately runs parallel to k_g. With increasing size, k_{HSA} converges rapidly against k_g. At $n = 100$, k_{HSA} is only 1.3% larger than k_g. k_{SCC} is consistently about twice as high as k_{HSA}. *Lower panel*: Fraction of molecules with $v \leq v_c$, whose collision rate is calculated with classical ADO capture theory. Already above a cluster sizes of $n = 10$, fewer than 5% of the molecules are slow enough that their capture radius is larger than the cluster. This reflects the weak interaction of the non-polar and only weakly polarizable He atom with the charged cluster.

executable of a small program for the calculation of HSA and SCC rate constants are available online (see Supplementary data), together with screenshots of the program which show the parameters used to generate Figs. 3–5.).

Although there are marked differences between the three examples, they have in common that already at a cluster size of $n = 10$, k_{ADO} is 5–60% smaller than k_{HSA}. The error is most pronounced for the weakly interacting He, for which the purely geometric collision dominated, which is the reason why He is used in ion mobility studies. For typical reactants in ion–molecule studies, ADO theory yields systematically too low collision rates for clusters.

A purely geometric collision cross section, however, deviates significantly from the HSA collision rate. For typical reactants in ion-molecule studies, neither k_{ADO} nor k_g come close to the value of k_{HSA} in a size region of $n = 5$–20. Even for He the deflection in the vicinity of the cluster is non-negligible, and for $n = 10$ k_{HSA} is 10% larger than k_g. This clearly illustrates that the effect of the long-range potential on the collision cross section can be significant for quite sizable clusters. A general rule, however, cannot be given, since both k_{HSA} and k_g critically depend on the mass and radius of the cluster.

The SCC rate illustrates the tremendous impact polarization and/or an asymmetric charge distribution can have on the collision rate. In all three examples, the SCC rate is about twice as high as the HSA rate, even for the seemingly weakly interacting helium atom.

The comparison with experiment is encouraging. For the reaction of hydrated electrons with CO_2 with clusters around $n = 50$, an efficiency $\Phi_{ADO} = k_{abs}/k_{ADO} = 300 \pm 75\%$ was estimated [25]:

$$(H_2O)_n^- + CO_2 \rightarrow CO_2(H_2O)_{n-m}^- + mH_2O \quad (19)$$

With the calculated HSA rate, this is reduced to $\Phi_{HSA} = k_{abs}/k_{HSA} = 160 \pm 40\%$, and the SCC rate yields $\Phi_{HSA} = k_{abs}/k_{HSA} = 74 \pm 18\%$. Not surprisingly, none of the two new rates yields perfect agreement with the experiment. However, comparison of the HSA and SCC rate together with the experimental result yields valuable insight: It is consistent with a charge distribution that is somewhat off-center or near the surface, but localized and not freely floating in the water cluster, and the assumption that the reaction occurs with collision frequency seems justified. It is suggested that for weakly polarizable clusters, the HSA and SCC rates provide lower and upper limits to the collision rate, respectively.

The situation is different in metal clusters. For strongly interacting reactants like CO, the HSA collision rate is only 3% larger than the ADO collision rate for the Pt_7^+ cluster. The most efficient reaction observed on Pt_7^+ was the burning of CO on $Pt_7O_2^+$, with an ADO efficiency of $\Phi_{ADO} = k_{abs}/k_{ADO} = 370 \pm 93\%$ [24]:

$$Pt_7O_2^+ + CO \rightarrow Pt_7O^+ + CO_2 \quad (20)$$

The SCC rate, however, yields a reaction efficiency of $180 \pm 45\%$, which is in better agreement with experiment. The disagreement can be rationalized by the non-spherical geometry of the cluster, or by a too conservative estimate of the cluster radius. The assumption of the SCC model that the neutral molecule modifies the charge distribution of the cluster and draws the charge to the surface seems eminently reasonable.

Figs. 6 and 7 show a more detailed comparison of previously published experimentally measured reaction rates of cobalt and rhodium clusters with CO with the newly esti-

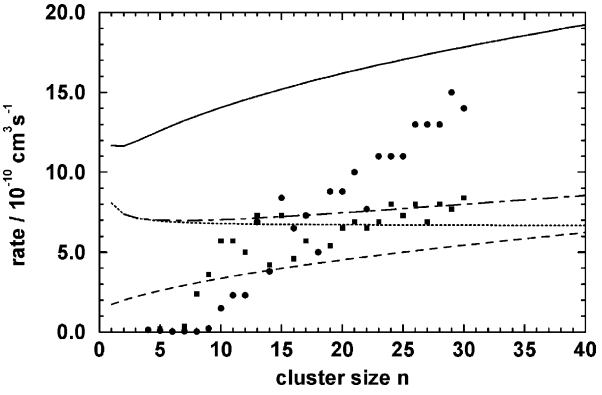

Fig. 6. Reaction $Co_n^{\pm}$ + CO. Hard sphere ADO rate k_{HSA} (dot-dashed line), Surface Charge Capture rate k_{SCC} (solid line), classical ADO collision rate k_{ADO} (dotted line), geometric collision rate k_g (dashed line), measured absolute rate constants for Co_n^+ (filled circles) and Co_n^- (filled squares). For all cluster sizes examined, k_{SCC} provides an upper limit to the experimental rate, while the other models are insufficient to explain the high rate constants. Experimental data are taken from ref. [29].

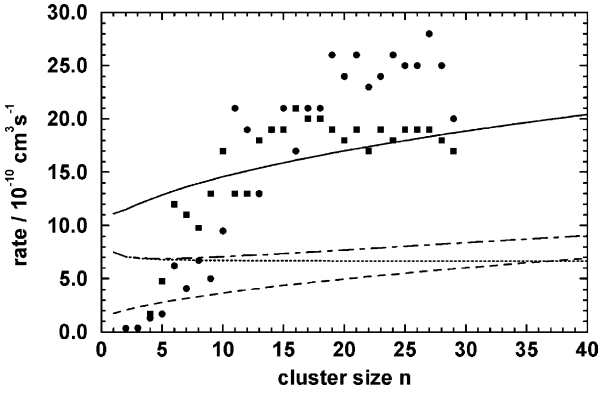

Fig. 7. Reaction $Rh_n^{\pm}$ + CO. Hard sphere ADO rate k_{HSA} (dot-dashed line), Surface Charge Capture rate k_{SCC} (solid line), classical ADO collision rate k_{ADO} (dotted line), geometric collision rate k_g (dashed line), measured absolute rate constants for Rh_n^+ (filled circles) and Rh_n^- (filled squares). In this case, the measured rate constants lie up to 50% higher than the k_{SCC} estimate, which suggests that a significantly asymmetric charge distribution is present, possibly induced by the CO reactant. Experimental data are taken from ref. [29].

mated collision rates [29]. For cobalt clusters, the SCC rate provides a firm upper limit to the measured reaction rates, indicating that charge delocalization is taking place to a significant extent. For rhodium, even the SCC rate is not capable of reproducing the highest measured rate constant, yielding a collision efficiency of 150% for CO attachment by Rh_{27}^+. Still, the differences between cobalt and rhodium can be rationalized with the higher polarizability of the latter, which is reflected in a higher gas phase reactivity of its ionic clusters towards CO attachment. In addition, the pronounced sensitivity of the collision rate towards the interaction potential suggests that the size-dependent reactivity may very well reflect the size-dependence of the polarizability and permanent dipole moment of the clusters. Recent studies on the electric properties of neutral niobium clusters [30] show that both polarizability and dipole moment show a pronounced size dependence.

4. Conclusion

Average dipole orientation theory can be modified to account for the finite size of ionic clusters in the calculation of collision rate constants. Even at moderate cluster sizes, the correction of ADO theory is significant. For weakly polarizable clusters like $(H_2O)_n^-$, the newly derived HSA rate constants lie significantly closer to experimentally measured rate constants than their ADO counterparts. For metal clusters, the SCC rate is usually more realistic. The models illustrate that the character of the collision between an ionic cluster and a neutral molecule changes from a capture collision to a hard sphere impact with increasing cluster size. This comparison provides valuable qualitative insight into the degree of charge localization and mobility in the ionic cluster. We suggest that for reactions that occur with collision rate, the size-dependent reactivity which is commonly observed for metal clusters reflects the size-dependence of the permanent dipole moment and the polarizability of the clusters.

Acknowledgements

Financial support from the Deutsche Forschungsgemeinschaft and the Fonds der Chemischen Industrie is gratefully acknowledged.

Appendix A. Supplementary data

Supplementary data associated with this article can be found, in the online version, at doi:10.1016/j.ijms.2005.03.012.

References

[1] T. Su, M.T. Bowers, J. Chem. Phys. 58 (1973) 3027.
[2] T. Su, M.T. Bowers, J. Am. Chem. Soc. 95 (1973) 1370.
[3] P. Langevin, Ann. Chim. Phys. 5 (1905) 245.
[4] A.I. Maergoiz, E.E. Nikitin, J. Troe, V.G. Ushakov, J. Chem. Phys. 105 (1996) 6263.
[5] A.I. Maergoiz, E.E. Nikitin, J. Troe, V.G. Ushakov, J. Chem. Phys. 105 (1996) 6270.
[6] A.I. Maergoiz, E.E. Nikitin, J. Troe, V.G. Ushakov, J. Chem. Phys. 105 (1996) 6277.
[7] W.J. Chesnavich, T. Su, M.T. Bowers, J. Chem. Phys. 72 (1980) 2641.
[8] T. Su, M.T. Bowers, Int. J. Mass Spectrom. Ion Phys. 12 (1973) 347.
[9] A.A. Shvartsburg, M.F. Jarrold, Chem. Phys. Lett. 261 (1996) 86.
[10] G. von Helden, M.T. Hsu, N. Gotts, M.T. Bowers, J. Phys. Chem. 97 (1993) 8182.
[11] J. Lermé, P. Dugourd, R.R. Hudgins, M.F. Jarrold, Chem. Phys. Lett. 304 (1999) 19.
[12] P. Weis, S. Gilb, P. Gerhardt, M.M. Kappes, Int. J. Mass Spectrom. 216 (2002) 59.
[13] M.F. Mesleh, J.M. Hunter, A.A. Shvartsburg, G.C. Schatz, M.F. Jarrold, J. Phys. Chem. 100 (1996) 16082.
[14] T. Wyttenbach, G. von Helden, J.J. Batka, D. Carlat, M.T. Bowers, J. Am. Soc. Mass Spectrom. 8 (1997) 275.
[15] P. Weis, O. Welz, E. Vollmer, M.M. Kappes, J. Chem. Phys. 120 (2004) 677.
[16] D.C. Clary, D. Smith, N.G. Adams, Chem. Phys. Lett. 119 (1985) 320.
[17] K. Sakimoto, Chem. Phys. Lett. 116 (1985) 86.
[18] K. Takayanagi, J. Phys. Soc. Jpn. 51 (1982) 3337.
[19] M. Quack, J. Troe, Ber. Bunsen-Ges. Phys. Chem. 79 (1975) 170.
[20] T. Su, J. Chem. Phys. 88 (1988) 4102.
[21] J. Troe, J. Chem. Phys. 87 (1987) 2773.
[22] S. Hu, T. Su, J. Chem. Phys. 85 (1986) 3127.
[23] T. Su, W.J. Chesnavich, J. Chem. Phys. 76 (1982) 5183.
[24] O.P. Balaj, I. Balteanu, M.K. Beyer, V.E. Bondybey, Angew. Chem. 116 (2004) 6681.

[25] O.P. Balaj, C.K. Siu, I. Balteanu, M.K. Beyer, V.E. Bondybey, Chem. Eur. J. 10 (2004) 4822.
[26] T. Schindler, C. Berg, G. Niedner-Schatteburg, V.E. Bondybey, Ber. Bunsen-Ges. Phys. Chem. 96 (1992) 1114.
[27] D. Schröder, H. Schwarz, D.E. Clemmer, Y.M. Chen, P.B. Armentrout, V.I. Baranov, D.K. Bohme, Int. J. Mass Spectrom. Ion Processes 161 (1997) 175.
[28] R.S. Berry, S.A. Rice, J. Ross, Physical Chemistry, Wiley, New York, 1980.
[29] I. Balteanu, U. Achatz, O.P. Balaj, B.S. Fox, M.K. Beyer, V.E. Bondybey, Int. J. Mass Spectrom. 229 (2003) 61.
[30] R. Moro, X.S. Xu, S.Y. Yin, W.A. de Heer, Science 300 (2003) 1265.